



Nonlinear Optical Effects in One Dimensional Multi-layer Structure Consisting of Polar Ferroelectric Called LiTaO_3

Omid Bahrami^{*,1}, Abdolrahim Baharvand¹

¹ Department of Physics, faculty of science, Lorestan University, Khorram-Abad, Lorestan, Iran

(Received 16 Dec. 2020; Revised 27 Jan. 2021; Accepted 16 Feb. 2021; Published 15 Mar. 2021)

Abstract: The transfer matrix method has been widely used to calculate the scattering of electromagnetic waves. In this paper, the second harmonic generation in finite size one-dimensional periodically poled LiTaO_3 has been investigated. To calculate the conversion efficiency, fundamental and second harmonic wave propagation among proposed structures, we use the transfer matrix method. In the designed nonlinear photonic crystal structure, the linear and nonlinear optical parameters are both periodically modulated, and thus the second harmonic generation efficiency can be several orders of magnitude larger than in a conventional quasi-phase matched nonlinear structure with the same sample length. The reason is that, due to the presence of photonic band gap edges, the density of states of the electromagnetic fields is large, the group velocity is small (as a result, the interaction time is increased), and the local field is enhanced. All three factors contribute to significant enhancement of the nonlinear optical interactions.

Keywords: Conversion Efficiency, Photonic Band Gap, Quasi-Phase Matching Conditions, Second Harmonic Generation.

1. INTRODUCTION

In recent years, amplification and increase of second harmonic generation (SHG) efficiency based on quasi-phase matching conditions (QPM) have been investigated in nonlinear photon crystals (NPCs) [1]. In order to establish the quasi phase matching conditions in periodic structures (photonic crystals), it is used to change the nonlinear polarization sign in the layers. In this method, the length of the layers should be correspond to the coherence length of the electromagnetic wave in the desired layer [2]. The method of changing the

* Corresponding author. Email: bahrami.om@fs.lu.ac.ir

nonlinear polarization sign in the layers is a suitable way for increasing conversion efficiency of the second harmonic [3].

The increase and amplification by several orders of magnitude of second harmonic generation efficiency in nonlinear photonic crystals has been investigated in ref [4, 5]. This increase and enhancement is due to the high density of resonant modes and the low speed of electromagnetic waves at frequencies near the photonic band gap (PBG) edge [4]. These factors are the reason for better enhancement and limitation of field (that means, for a certain range of radiation electromagnetic frequencies, the conversion efficiency is high) [6].

In recent decades, ferroelectric crystals with periodic polarization have been considered due to the unique properties that have been used to compensating for the phase mismatch in nonlinear optical interaction processes. Second-order nonlinear optical interaction, for example, second harmonic generation (SHG) and the optical parametric oscillator, has been investigated in structures composed of periodic polarized ferroelectric such as LiNbO_3 , KTiOPO_4 and SBN ($\text{Sr}_x\text{Ba}_{1-x}\text{Nb}_2\text{O}_6$, $0.32 \leq x \leq 0.82$) [7-11]. However, it's always difficult to achieve high-power nonlinear radiation, because there are always optical losses.

In recent years, increasing the nonlinear conversion efficiency in ferroelectric crystals with periodic polarization has been a long term objective. Lately, an increase by several orders of magnitude of second-order nonlinear conversion efficiency in these photonic crystals has been reported in [12]. This increase, as we have said, is related to the high density of resonance modes and the low velocity of electromagnetic waves at frequencies near the photonic band gap edge.

In addition, the theoretical analysis of the second harmonic generation has been investigated in multilayered structures in [13]. However, the impact of the band gap edge (high density of resonant modes and low velocity of electromagnetic waves) has not been considered in ferroelectric structures composed of LiTaO_3 with periodic polarization. In this paper, we consider the second harmonic generation (SHG) in nonlinear crystals including LiTaO_3 with periodic polarization with different refractive indices using the transfer matrix method.

In this paper, we use the transfer matrix method in order to investigate the SHG problem in nonlinear multi-layered systems in which fundamental plane-wave beams incident vertically to the surface of the structure, and so that both linear and nonlinear properties alternate throughout the system. It is assumed that nonlinear optical processes are weak so that the fundamental pump waves are not necessarily affected by the nonlinear process. Using this method, we calculate not only the second harmonic wave energy in the output of structure, but also the distribution of the pump and the second harmonic fields within the system. In our method, there is no approximation except for the non-depleted pump wave

approximation. The results of this paper are different from the results of the works in which the systems is based only on the traditional quasi-phase matching (QPM). We will discuss the cause of this difference in the following.

This paper is organized as follows in sec.II we focus on the details of the model and we derive the related transfer matrix. We also explain how we calculate the conversion efficiency. In sec.III we present and discuss our numerical results. Finally, sec. IV ends the paper with a summary of our results.

2. MODEL AND METHOD

In this section, we study a multi-layered nonlinear structure, which changes the nonlinear parameter sign periodically in layers. In this structure, the scales of linear and nonlinear parameters are the same (We followed the methods of bahrami et al. 2019 in ref [14]). The nonlinear structure is divided into N periods of thickness d , and each period is divided into two homogeneous sections, Fig. 1. Thickness and linear parameter (refractive index) and nonlinear parameter (second order susceptibility) for section I are, respectively, d_I , $n_I^{(r)}$ and $\chi^{(2)}$, while those for section II are, d_{II} , $n_{II}^{(r)}$ and $-\chi^{(2)}$, while $r = f, s$ is use for the fundamental field and second harmonic field, respectively. Due to the fact that the refractive index of regions I ($n_I^{(r)}$) and II ($n_{II}^{(r)}$) are not equal, Its reflection will occur at each layer interface, resulting in between the transmitted and reflective waves in each layer, The phenomenon of interference will appear.

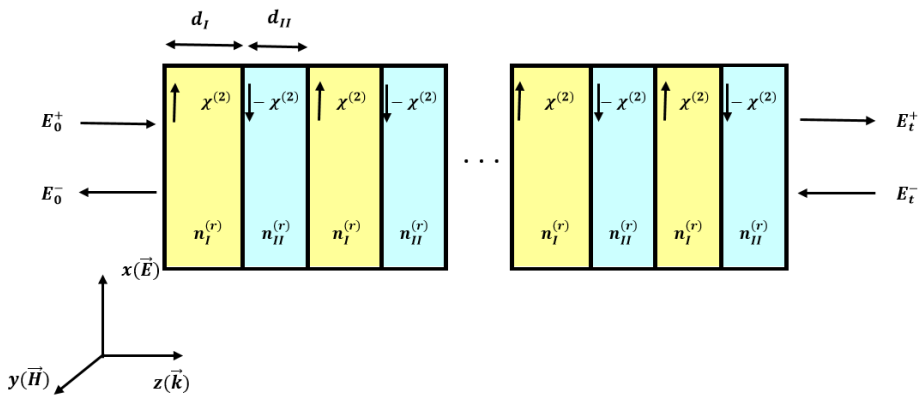


Fig. 1. Multi-layered nonlinear structure. In each layer, the vectors represent the nonlinear polarization direction.

It is assumed that an electromagnetic wave with frequency ω incident from the left-hand side of the system and propagates in the direction of the z axis, so that the polarization of the electric field is in the x -axis direction. Our numerical calculations are based on the nonlinear transfer matrix method (TMM) [15, 16]. In this method, the SHG process is divided into three stages: (1) First, the fundamental field (FF), with the propagation in the structure, causes the macroscopic polarization of matter. (2) Since the material is non-linear, then the second-order nonlinear polarization is created in matter. And this nonlinear polarization radiates the second harmonic (SH) field in the structure. (3) This second harmonic field is propagated in the device, and it comes out in the form of a second harmonic signal.

In the first stage of the second harmonic generation, the fundamental and second harmonic fields follow the following equations:

$$\begin{aligned}\nabla \times (\nabla \times \vec{E}_{2\omega}) - \frac{\varepsilon_{2\omega}(2\omega)^2}{c^2} \vec{E}_{2\omega} &= \mu_0(2\omega)^2 \vec{P}_{NL}^{2\omega} \\ \nabla \times (\nabla \times \vec{E}_\omega) - \frac{\varepsilon_\omega \omega^2}{c^2} \vec{E}_\omega &= \mu_0 \omega^2 \vec{P}_{NL}^\omega\end{aligned}\quad (1)$$

In which, ε_ω , $\varepsilon_{2\omega}$, \vec{P}_{NL}^ω , and $\vec{P}_{NL}^{2\omega}$ are permittivity and nonlinear polarization at *FF* and *SH* frequencies. Because the nonlinear process is weak, As a result, the nonlinear process has no significant effect on the intensity of the fundamental pump field. So here we are using the non-depleted pump wave approximation, $E_{2\omega} \ll E_\omega$. Therefore, the above equations for the m -th layer are as follows

$$\begin{aligned}\left[\frac{d^2}{dz^2} + (k_m^{(f)})^2 \right] E_m^f(z) &= 0 \\ \left[\frac{d^2}{dz^2} + (k_m^{(s)})^2 \right] E_m^s(z) &= -\mu_0(2\omega)^2 \vec{P}_{NL}^{2\omega}\end{aligned}\quad (2)$$

Where $k_m^{(f)} = n_m^{(f)} k_0^{(f)}$, $k_m^{(s)} = n_m^{(s)} k_0^{(s)}$, $k_0^{(f)} = \omega/c$, and $k_0^{(s)} = 2\omega/c$. and also, $n_m^{(f)}$ and $n_m^{(s)}$ show the refractive index of the pump waves and the second harmonic, respectively in the m th slab; c , the speed of light is in vacuum. The first equation of coupling equations (2) gives the fundamental electric field in the m th layer.

$$E_m^{(f)} = E_m^{f+} e^{i(k_m^{(f)}(z-z_{m-1})-\omega t)} + E_m^{f-} e^{-i(k_m^{(f)}(z-z_{m-1})-\omega t)} \quad (3)$$

Where z_0 is zero, $z_m = z_{m-1} + d_m$ and d_m is the thickness of the m th layer. $E_m^{(f)+}$ is the magnitude of forward plane wave and $E_m^{(f)-}$ is the magnitude of backward plane wave at the left interface of the m th layer.

According to the continuity conditions on the boundary of the layers, we have the following matrix relation between the electric and magnetic fields passing through odd layer to even layer:

$$\begin{pmatrix} E_{2m-1}^{f+} \\ E_{2m-1}^{f-} \end{pmatrix} = \frac{1}{2n_I^{(1)}} \begin{pmatrix} n_I^{(1)} + n_{II}^{(1)} & n_I^{(1)} - n_{II}^{(1)} \\ n_I^{(1)} - n_{II}^{(1)} & n_I^{(1)} + n_{II}^{(1)} \end{pmatrix} \begin{pmatrix} E_{2m}^{f+} \\ E_{2m}^{f-} \end{pmatrix} = T_{12} \begin{pmatrix} E_{2i}^{f+} \\ E_{2i}^{f-} \end{pmatrix} \quad (4)$$

Using the matrix of dynamics and the matrix of propagation that are as follows.

$$D_m = \begin{pmatrix} 1 & 1 \\ n_m^{(f)} & -n_m^{(f)} \end{pmatrix}$$

$$P_m = \begin{pmatrix} \exp(ik_m^{(f)} d_m) & 0 \\ 0 & \exp(-ik_m^{(f)} d_m) \end{pmatrix}$$

The general transfer matrix for the multi-layer structure is as follows

$$T = D_0^{-1} (D_{II} P_{II} D_{II}^{-1} D_I P_I D_I^{-1})^N D_0 \quad (5)$$

This transfer matrix connects the fields at the beginning and the end of the structure, as follows

$$\begin{pmatrix} E_t^{f+} \\ E_t^{f-} \end{pmatrix} = T \begin{pmatrix} E_0^{f+} \\ E_0^{f-} \end{pmatrix} \quad (6)$$

For harmonic fields that is produced in the structure, we use equation (2) with

$P_{NL}^{2\omega}(z, t) = \varepsilon_0 \chi_m^{(2)} [E_m^{(f)}(z)]^2 \exp(-i2\omega t)$ that yields to:

$$\begin{pmatrix} E_m^{(s)+} \\ E_m^{(s)-} \end{pmatrix} = G_0^{-1} S G_0 \begin{pmatrix} E_{m-1}^{(s)+} \\ E_{m-1}^{(s)-} \end{pmatrix} + G_0^{-1} (N_{II} B_I F_I - S B_I) A_I \begin{pmatrix} (E_{2m-1}^{f+})^2 \\ (E_{2m-1}^{f-})^2 \end{pmatrix}$$

$$+ G_0^{-1} (N_{II} - S) \begin{pmatrix} C_I E_{2m-1}^{f+} E_{2m-1}^{f-} \\ 0 \end{pmatrix} + G_0^{-1} (B_{II} F_{II} - N_{II} B_{II}) A_{II} \begin{pmatrix} (\Omega_{2m}^+)^2 \\ (\Omega_{2m}^-)^2 \end{pmatrix}$$

$$+ G_0^{-1} (I - N_{II}) \begin{pmatrix} C_{II} E_{2m}^{f+} E_{2m}^{f-} \\ 0 \end{pmatrix} \quad (7)$$

In which:

$$A_l = \frac{-4\mu\varepsilon_0 \chi_l^{(2)} \omega^2}{k_l^{(s)2} - 4k_l^{(f)2}}, \quad C_l = \frac{-4\mu\varepsilon_0 \chi_l^{(2)} \omega^2}{k_l^{(s)2}}$$

$$G_l = \begin{pmatrix} 1 & 1 \\ n_l^{(s)} & -n_l^{(s)} \end{pmatrix}, \quad B_l = \begin{pmatrix} 1 & 1 \\ \frac{2k_0^{(f)} n_l^{(f)}}{k_0^{(s)}} & -\frac{2k_0^{(f)} n_l^{(f)}}{k_0^{(s)}} \end{pmatrix}$$

$$Q_l = \begin{pmatrix} \exp(ik_l^{(s)} d_l) & 0 \\ 0 & \exp(-ik_l^{(s)} d_l) \end{pmatrix}$$

$$F_l = \begin{pmatrix} \exp(i2k_l^{(f)} d_l) & 0 \\ 0 & \exp(-i2k_l^{(f)} d_l) \end{pmatrix} \quad l = I, II$$

$$S = G_{II} Q_{II} G_{II}^{-1} G_I Q_I G_I^{-1}, \quad N_{II} = G_{II} Q_{II} G_{II}^{-1}$$

In this section, we determined the method of obtaining the amplitude of the second harmonic field in the nonlinear multi-layer structure. We can not actually measure this quantity, but the intensity of the second harmonic is measurable. Using the intensity of waves, we have the following definitions for the transmitting conversion efficiency and the reflecting conversion efficiency:

$$\eta_t = \frac{I_{harm}^t}{I_{pump}}$$

$$\eta_r = \frac{I_{harm}^r}{I_{pump}} \quad (8)$$

Where $I_{harm}^{t,r}$ and I_{pump} are the intensities of the reflected or transmitted harmonic and pump fields, respectively.

In our 1DCROW structure, it is assumed that the nonlinear photonic crystal are composed of periodically poled lithium tantalite (LiTaO₃) crystal, whose nonlinear susceptibility is $\chi^{(2)} = 13.8$ pm/V and The refractive index for lithium tantalite (LiTaO₃) is given by the following dispersion formula [17]:

$$n^2(\lambda, T) = A + \frac{B + b(T)}{\lambda^2 - [C + c(T)]^2} + \frac{E}{\lambda^2 - F^2} + D\lambda^2 \quad (9)$$

Where $A = 4.5284$, $B = 7.2449 \times 10^{-3}$, $C = 0.2453$, $D = -2.3670 \times 10^{-2}$, $E = 7.7690 \times 10^{-2}$, $F = 0.1838$, $b(T) = 2.6794 \times 10^{-8}(T + 273.15)^2$, $c(T) = 1.6234 \times 10^{-8}(T + 273.15)^2$.

Periodic polar ferroelectric (LiTaO₃) crystals are described by modulations of the nonlinear susceptibilities. An optoelectronic effect is used to produce the photonic band gap structure. This effect is the origin of the modulation of the refractive index of the layers in the photonic crystal. If the electric field E is applied in the direction of the optical axis of the material, correction of refractive index and new refractive index (in odd layers) are as follows:

$$n_I = n + \Delta n_I = n - \frac{1}{2}n^3r_{33}E \quad (10)$$

Where r_{33} is the optoelectronic coefficient of the material and E is the electric field amplitude. Similar to the nonlinear optical coefficient, the optoelectronic coefficient of the material in different layers has different signs. So in reverse (even) layers the optoelectronic coefficient changes sign and the refractive index in these layers is written as follows:

$$n_{II} = n + \Delta n_{II} = n + \frac{1}{2}n^3r_{33}E \quad (11)$$

It is obvious that a modulated linear susceptibility occurs due to the presence of an external strong electric field based on the electro-optical effect. As a result, photonic band gaps may become available in periodically poled ferroelectric crystals. If there is only a modulation of nonlinear susceptibility while the linear refractive indices are uniform, the conversion efficiency will be modulated by the phase difference between the FF and SH field. The maximal conversion efficiency will be achieved when the quasi-phase-matched condition is satisfied. But when there are large refractive index discontinuities, the phase of the transmitted plane-wave field will undergo a shift at the boundary. The wave vectors are also strongly modified because of the appearance of photonic band

gaps. As a result, the original QPM condition is violated and the conventional QPM mechanism must be rewritten in the new nonlinear photonic crystal structures. Although a Bloch wave can be defined in this structure, which has a periodic refractive index modulation, and with the non depleted pump wave approximation the FF can be represented by the Bloch wave, yet for the generated SH wave, a Bloch wave representation is inappropriate for several reasons. First, the forward Bloch wave is subject to reflection at the sample surface. More importantly, the SH wave radiated from the nonlinear polarization created by the Bloch wave will encounter significant multiple reflection within the remarkably modulated photonic crystal structure. Finally, the SH wave is also subject to reflection at the sample surface. It is then clear that a Bloch wave is not the most appropriate tool to accurately describe the nonlinear optical interactions in the current structure. It is very difficult to extract an explicit expression for the phase match condition from such a picture.

3. NUMERICAL RESULTS

From the relatively heavy mathematical calculations of Sec.II, it is clear that the existence of a strong light scattering effect in the structure of the photonic crystal complicates the analysis of the second harmonic generation problem. It is obvious that the conventional analytical solution is used to the ordinary quasi-phase matching (QPM) problem is no longer applicable. Therefore, numerical simulation is used to establish QPM conditions in the nonlinear multi-layer structure. We do this by adjusting the thickness of the two constituent parts of the structure. Quasi-phase matching conditions and optimal structure occur at the maximum conversion efficiency. In Fig. 2, the frequency conversion efficiency of SH as a function of the thickness of each part (d) is plotted so that the width of the positive region (The positive region is a region in which $\chi^{(2)}$ is positive) is $d_1 = 3000nm$.

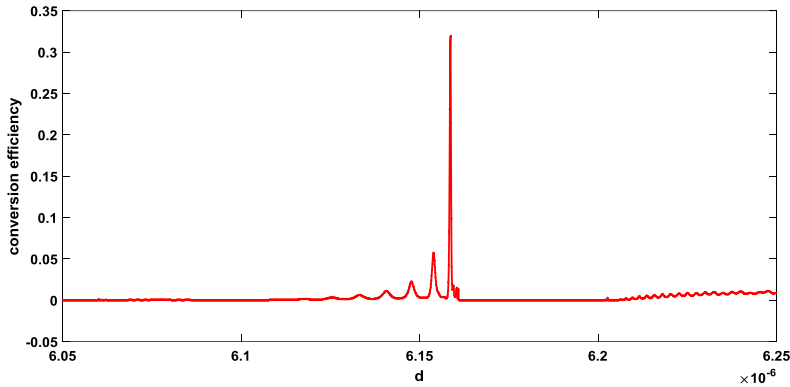


Fig. 2. Conversion efficiency of SH wave in terms of thickness of each part, d the peak of conversion efficiency happens when $d = 6158.7nm$ and $d_l = 3000nm$. The wavelength of the fundamental wave is $\lambda = 1064 nm$.

The structure consists of 35 pairs of layers and the initial wavelength (pump) is 1064 nm. In this wavelength, the refractive indices of the positive and negative regions are $n_I^{(f)} = 1.0846$ and $n_{II}^{(f)} = 1.8193$, respectively. The intensity of the external electric field is of the order of tens of kV/mm . The refractive indices for the SH wave in the positive and negative regions are $n_I^{(s)} = 1.0387$ and $n_{II}^{(s)} = 1.8653$, respectively. According to Fig. 2, the maximum conversion efficiency occurs at $d = 6158.7nm$.

As we know, the second harmonic conversion efficiency, in addition to being dependent on the power of the pump light, also strongly depend on intensity of the pump light inside the structure. So, in addition to the QPM conditions, the properties of the photonic band edges in amplifying and increasing the SH conversion efficiency are very effective. Figure 3 shows the SH conversion efficiency as a function of fundamental field intensity.

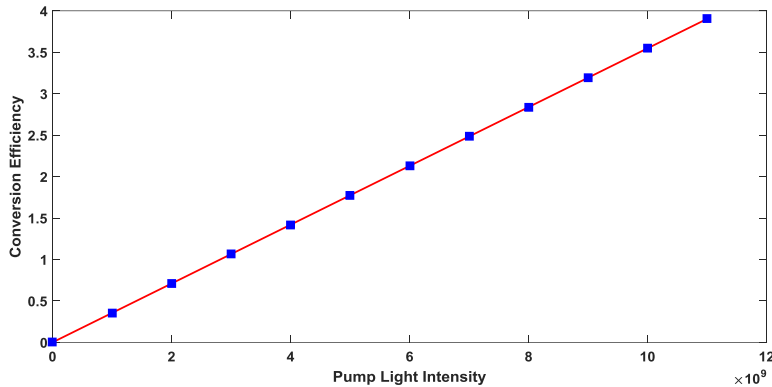


Fig. 3. The SH wave efficiency vs fundamental wave intensity of the pump. The squares represent the calculated values and the red line represents the linear fit of the points. The structure is the same as the structure of Fig. 2.

As we said, the conversion efficiency is defined as the ratio of the second harmonic intensity to the pump intensity. For comparison, the SH conversion efficiency of a uniform lithium tantalite (LiTaO_3) crystal (the crystal with fixed second-order susceptibility coefficient $\chi^{(2)}$) with quasi-matching matching conditions, which is longitudinally equal to the length of the investigated structure in this paper, as shown in Figure 4. The order of magnitude of the convergence efficiency in Fig. 4 is about 10^{-4} , which is four times smaller than the conversion efficiency in the designed structure (Fig. 3).

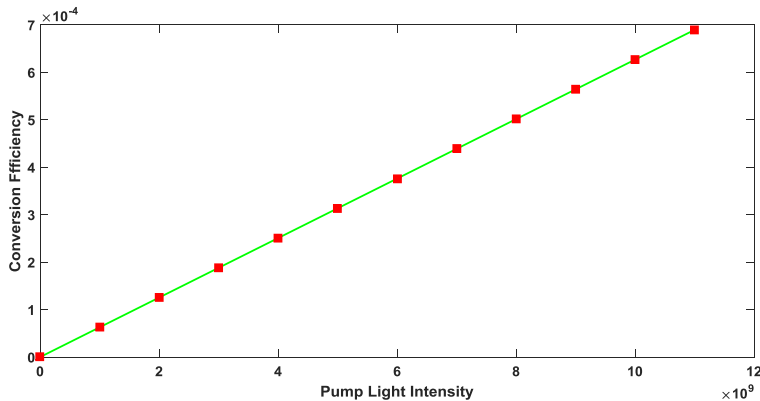


Fig. 4. The SH wave efficiency vs fundamental wave intensity of the pump for uniform lithium tantalite (LiTaO_3) crystal. The squares represent the calculated values and the green line represents the linear fit of the points.

The calculated transmission spectrum for $d = 6158.7\text{nm}$ is shown in Fig. 5. By selecting these parameters (refractive index of layers and width of layers) for the nonlinear system, the FF and SH signals are all located at the photonic band gap edges. At the edge of the gap, the density of the electromagnetic waves is large and the group velocity of the wave is small. As a result, the domain of the field increases by several order of magnitude, and the time of nonlinear interaction becomes much larger. The combination of these factors is the main reason for the significant improvement in SH conversion efficiency.

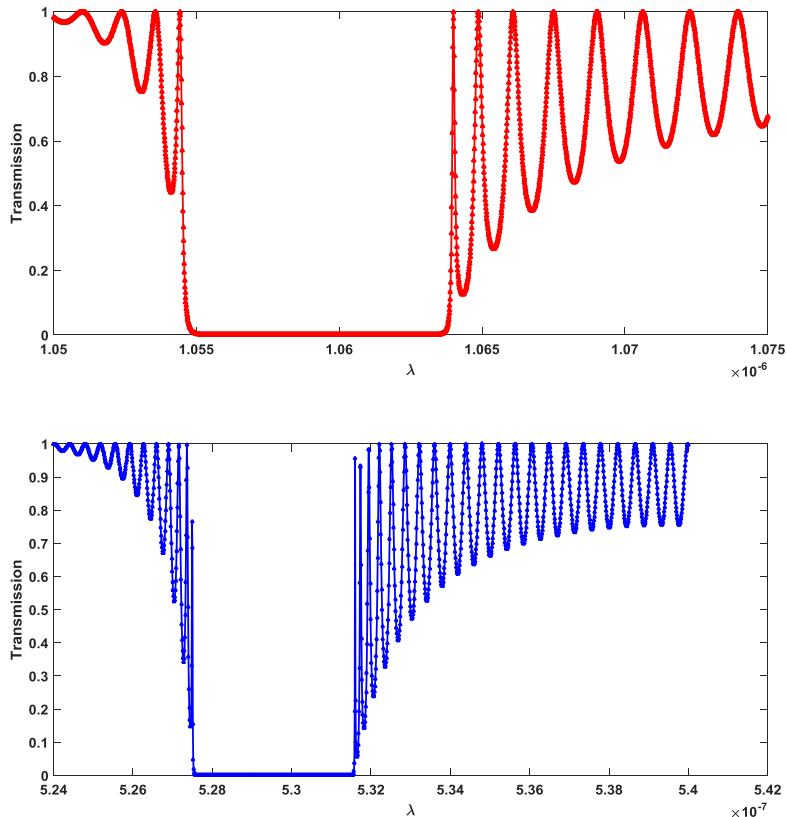


Fig. 5. The transmission spectrum in the vicinity of the pump wavelength (red) and the second harmonic wavelength (blue) when $d = 6158.7\text{nm}$ for the optimal structure that produces the second harmonic waves is shown in Fig.2

In Figure 6, the SHG conversion efficiency is plotted in terms of wavelength in the vicinity of the pump wavelength (1064nm). The photonic crystal structure of Figure 6 is similar to Fig. 5. The upper and lower shapes indicate the intensity of the backward (reflective) and forward (passing) output, respectively. The conversion efficiency values in Fig. 6 are normalized to unity. It is clear from Figure 6 that the desired structure effectively radiates the second harmonic signals in both directions (forward and backward). The intensity of the backward SH signal is large and is approximately equal to the intensity of the forward SH signal. But in a bulk nonlinear optical material with only phase-matching conditions, which is longitudinally equal with the structure studied in this paper, the backward signal is smaller one or more orders of magnitude than the forward signal. The wavelength of the maximum signal SH, in Fig. 6, corresponds to the wavelength of the band gap edge in Figure 5.

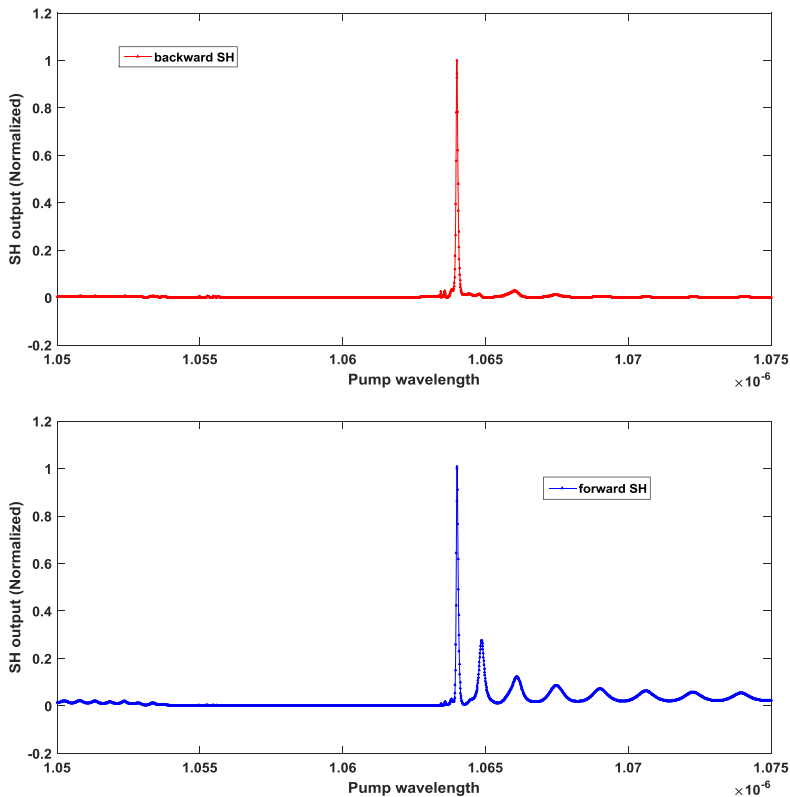


Fig. 6. SH signal (normalized) in terms of initial wavelength. The parameters of the system with the parameters of the structure of Figure 5 are the same.

The distribution of the pump field inside the nonlinear system is calculated by the transfer matrix method (TMM) and is shown in Fig. 7. Regarding the shape, due to the interference induced by multiple reflections, we can observe the pump field that oscillates within the structure, the maximum intensity is increased by one or more order of magnitude than the intensity of the collision field (the field at the beginning of the structure).

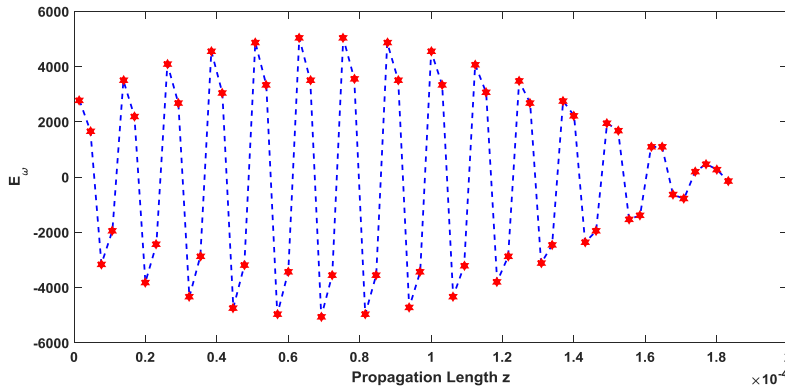


Fig. 7. Distribution of pump wave intensity within nonlinear structure at wavelength 1064 nm. The intensity of the pump field doubles as compared with the input wave at the beginning of the structure ($z = 0$).

4. CONCLUSION

In summary, we have developed a transfer matrix method to analyze the SHG problem in multilayered nonlinear optical media. Multiple reflection and interference effects are taken into account while deriving the transfer matrix for both the fundamental and SH waves. The proposed method is free from the several major approximations made in the previous literature that handled the harmonic generation problem in conventional QPM nonlinear optical media. To this extent, it is an exact approach and can give accurate results using the method, we have investigated the radiation of SH waves from both sides of a nonlinear optical sample and the distribution of SH fields within the structure. As an example, we have investigated SHG in a one-dimensional LiTaO_3 nonlinear photonic crystal. Comparison has been made between the current designed and the conventional QPM structure. It is found that, in an optimum structure, the second harmonic generation efficiency can be several orders of magnitude larger than in a conventional QPM nonlinear structure with the same sample length. The reason is that, due to the presence of photonic band gap edges, the density of states of the electromagnetic fields is large, the group velocity is small, and the local

field is enhanced. All three factors contribute to the significant enhancement of nonlinear optical interactions. In addition to the usual SHG from the forward direction of the pump wave, the SHG from the backward direction is also strong due to the large scattering effect by the nonlinear photonic crystal.

REFERENCES

- [1] Yasaman Abed, Fatemeh Mostaghni, *Polarizability and Hyperpolarizability of Schiff Base Salen-H2 as Judged as UV-vis Spectroscopy and Simulation Analysis*, Journal of Optoelectrical Nanostructures, Vol. 3, No. 1, Winter 2018.
- [2] Behnam Kazempour, Fatemeh Moslemi, *Adjustable Three Color Optical Filters Using Ferroelectric -Dielectric Generalized Heterostructures Photonic Crystals*, Journal of Optoelectrical Nanostructures, Vol. 5, No. 1, Winter 2020.
- [3] Tahmineh Jalali, Abdolrasoul Gharaati, Mohammad Rastegar, Mohammad Ghanaatian, *Enhancement of the Magneto-Optical Kerr Effect in One-Dimensional Magnetophotonic Crystals with Adjustable Spatial Configuration*, Journal of Optoelectrical Nanostructures, Vol. 4, No. 1, Winter 2019.
- [4] Momchil Minkov, Dario Gerace, and Shanhui Fan, *Doubly resonant $\chi^{(2)}$ nonlinear photonic crystal cavity based on a bound state in the continuum*, Optica, Vol. 6, Issue 8, pp. 1039-1045, 2019.
- [5] M.L. Ren, Z.Y. Li, *Enhanced nonlinear frequency conversion in defective nonlinear photonic crystals with designed polarization distribution*, J. Opt. Soc. Am. B 27, 1551, 2010.
- [6] M.L. Ren, Z.Y. Li, *High conversion efficiency of second harmonic generation in a short nonlinear photonic crystal with distributed Bragg reflector mirrors*, Appl. Phys. A 107, 71, 2012.
- [7] P. Xu, S. H. Ji, S. N. Zhu, X. Q. Yu, J. Sun, H. T. Wang, J. L. He, Y. Y. Zhu, and N. B. Ming, *Conical Second Harmonic Generation in a Two-Dimensional $\chi^{(2)}$ Photonic Crystal: A Hexagonally Poled LiTaO₃ Crystal*, Phys. Rev. Lett. 93, 133904, 2004.
- [8] P. Ni, B. Ma, X. Wang, B. Cheng, and D. Zhang, *Second-harmonic generation in two-dimensional periodically poled lithium niobate using second-order quasi phase matching*, Appl. Phys. Lett. 82, 4230, 2003.

- [9] L. E. Myers, R. C. Eckardt, M. M. Fejer, and R. L. Byer, *Quasi-phase-matched optical parametric oscillators in bulk periodically poled LiNbO₃*, J. Opt. Soc. Am. B 12, 2102.
- [10] TianXin Wang, PengCheng Chen, Chuan Xu, ShiNing Zhu, *Periodically poled LiNbO₃ crystals from 1D and 2D to 3D*, Science China Technological Sciences 63(7), May 2020.
- [11] Mousa Ayoub, Jörg Imbrock, and Cornelia Denz, *Ferroelectric domain diagnostics near the phase transition by Čerenkov second-harmonic generation*, Optical Materials Express, Vol. 7, Issue 9, pp. 3448-3455, 2017.
- [12] G. Vecchi, J. Terres, D. Coquillat, and M. L. V. d'Yerville, *Enhancement of visible second-harmonic generation in epitaxial GaN-based two-dimensional photonic crystal structures*, Appl. Phys. Lett. 84, 1245, 2004.
- [13] Hammid AL-Ghezi, Rudra Gnawali, Partha P. Banerjee, Lirong Sun, Jonathan Slagle, and Dean Evans, *2 × 2 anisotropic transfer matrix approach for optical propagation in uniaxial transmission filter structures*, Optics Express, Vol. 28, Issue 24, pp. 35761-35783, 2020.
- [14] B. Omid, B. Abdolrahim, and B. Ali, *Disorder Effect on the Transmission of Second Harmonic Waves in One-Dimensional Periodically Poled LiTaO₃*, Journal of Modern Physics, Vol.10 No.4, March 2019.
- [15] P. M. Bell, J. B. Pendry, L. Marin Moreno, and A. J. Ward, *A program for calculating photonic band structures and transmission coefficients of complex structures*, Comput. Phys. Commun. 85, 306, 1995.
- [16] L. L. Lin, Z. Y. Li, and K. M. Ho, *Lattice symmetry applied in transfer-matrix methods for photonic crystals*, J. Appl. Phys. 94, 811, 2003.
- [17] Lei Wang, Xintong Zhang, Lingqi Li, Qingming Lu, Carolina Romero, Javier R. Vázquez de Aldana, and Feng Chen, *Second harmonic generation of femtosecond laser written depressed cladding waveguides in periodically poled MgO:LiTaO₃ crystal*, Optics Express, Vol. 27, Issue 3, pp. 2101-2111, 2019.